Simulation Study of Body Surface RF Propagation for UWB Wearable Medical Sensors

Wen-Bin Yang, Kamran Sayrafian-Pour, John Hagedorn, Judith Terrill
Information Technology Laboratory
National Institute of Standards and Technology
Gaithersburg, Maryland, USA
{wyang, ksayrafian, hagedorn, Judith.terrill}@nist.gov

Kamya Yekeh Yazdandoost
Medical ICT Institute
New Generation Wireless Communications Research Center
National Institute of Information and Communications Technology
Yokosuka, Japan
yazdandoost@nict.go.jp

Abstract — **Ultra Wide-Band (UWB) is a favorable technology for wearable medical sensors that monitor vital signs and other health-related information. Efficient transceiver design requires in-depth understanding of the propagation media which in this case is the human body surface. The results of the few measurement experiments in recent publications point to varying conclusions in the derived parameters of the channel model. As obtaining large amount of data for many scenarios and use-cases is difficult for this channel, a detailed simulation platform can be extremely beneficial in highlighting the propagation behavior of the body surface and determining the best scenarios for limited physical measurements. In this paper, an immersive visualization environment is presented, which is used as a scientific instrument that gives us the ability to observe three-dimensional RF propagation from wearable medical sensors around a human body. We have used this virtual environment to further study UWB channels over the surface of a human body. Parameters of a simple statistical path-loss model and their sensitivity to frequency and the location of the sensors on the body are discussed.**

Keywords – Channel model; Ultra-WideBand (UWB); Immersive visualization system; Body Area Networks

I. INTRODUCTION

Body Area Networks (BAN) which consist of RF-enabled wearable and implantable sensory nodes are poised to be a promising interdisciplinary technology with novel uses in pervasive health information technology. However, numerous challenges including size, cost, energy source, sensing/actuator technology, transceiver design still need to be resolved [4]. RF-enabled wearable sensor nodes offer an attractive set of applications, among which we can point to Electrocardiogram (ECG), various medical monitoring applications such as Temperature, Respiration, Heart rate, Blood pressure and pH.

Recent advances in microelectronics indicate that the technology to achieve ultra-small and ultra low power wearable devices is mostly available. Successful adoption of these devices heavily depends on the existence of a global standard for their communication link (i.e., air interface). This is clearly due to the nature of their medical applications. UWB seems to be a favorable candidate frequency band in the radio spectrum that is almost universally available. Although, factors such as interference and co-existence with other wireless technologies are extremely important in the choice for BAN operating frequency, worldwide availability (i.e., partially) and also the opportunity to have reasonable (i.e., small) sized antennas make UWB an attractive candidate for wearable BAN applications.

Efficient transceiver design requires in-depth understanding of the propagation media which in this case is human body surface. The results of the few measurement experiments in recent publications point to varying conclusions in the derived parameters of the channel model. For example, authors in [8] perform measurement between a receiver node located on the stomach and 9 transmitter nodes that are placed around the front-upper side of the body. Their obtained average path loss exponent for UWB is around 0.84. Authors in [9] conduct measurement around the human torso in various parallel planes and obtain a path-loss exponent of around 5.8. Path-loss exponents of around 3 have also been reported when measurements are performed in front of the torso [10,11]. These discrepancies simply point to the need for more detailed studies in order to understand the behavior of Radio Frequency (RF) waves over the human body surface.

As obtaining large amount of data for many scenarios and use-cases for this channel is difficult, a platform that can emulate physical experiments in a three-dimensional (3D) virtual reality environment can be extremely beneficial in highlighting the propagation behavior of the body surface; and also determining the best scenarios for limited physical measurements. Lack of a detailed human body model and a realistic wearable antenna are usually among the shortcomings of previous simulation studies in this area.

In this paper, we use a sophisticated and innovative 3D virtual reality simulation platform to study electromagnetic propagation from wearable sensors. Communication with a wearable device can be done from any direction inside, outside or over the surface of the body due to various body postures and human motion. Consequently, a true 3D environment is needed to better capture, visualize and understand RF propagation for such devices. In the following sections, we describe such a platform and show how it can be used to

extract a simple statistical path-loss model for body surface communication.

The rest of this paper is as follows. Section 2 will describe the immersive 3D platform that we have constructed to study RF propagation from wearable sensors. The antennas used in our simulations are discussed in section 3. Then, description of the simulated scenarios and our results are provided in Section 4. Finally concluding remarks and future plans are expressed in Section 6.

II. A 3D VISUALIZATION SYSTEM FOR WEARABLE & IMPLANTABLE SENSORS

Figure 1 shows the block diagram of our simulation system. As observed, the main components of this system include: a three-dimensional human body model, the propagation engine which is a three-dimensional full-wave electromagnetic field simulator (i.e., HFSS[1]) and the 3D immersive & visualization platform. The 3D human body model includes frequency dependent dielectric properties of 300+ parts in a male human body. These properties are also user-definable if custom changes or modifications are desired. The human body model has a resolution of 2 mm. The HFSS propagation engine enables us to compute a variety of different electromagnetic quantities such as the magnitude of electric and magnetic fields Poynting vectors, and Specific Absorption Rate (SAR).

The 3D immersive platform as shown in Fig. 2 includes several components: three orthogonal screens that provide the visual display, the motion tracked stereoscope glasses, and the hand-held motion tracked input device. The screens are large projection video displays that are placed edge-to-edge in a corner configuration. These three screens are used to display a single three-dimensional stereo scene. The scene is updated based on the position of the user as determined by the motion tracker. This allows the system to present to the user a 3D virtual world within which the user can move and interact with the virtual objects. The main interaction device is a hand-held three button motion-tracked wand with a joystick.

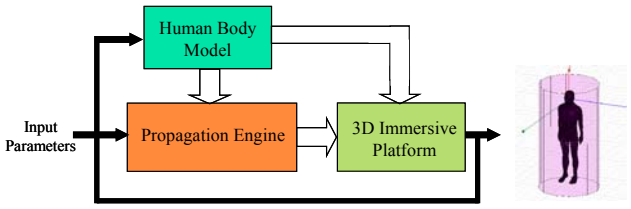

Figure 1. System block diagram

This virtual environment allows for more natural interaction between experts with different backgrounds such as engineering and medical sciences. The user can look at data representations at any scale and position, move through data, change orientation, and control the elements of the virtual world using a variety of interaction techniques including measurement and analysis [1]. All of these capabilities are extremely useful when studying RF propagation for wearable or implantable medical sensors [7].

Input parameters to our system include: a wearable antenna (i.e. its characteristics, exact position on the body and its orientation), operating frequency, transmit power, resolution, range and the choice of the desired output parameter. Resolution of 4 mm has been selected to run the simulations in this study.

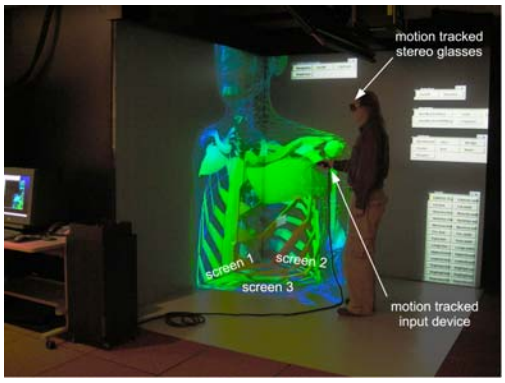

Figure 2. A User in the NIST Immersive Visualization Environment

III. A UWB ANTENNA FOR WEARABLE MEDICAL SENSORS

Antenna is a key component of wireless body area network. There exist many technical challenges in designing appropriate antennas for BAN. Biocompatibility and size-limitation from one side and bandwidth, efficiency and gain within the limited antenna volume are among many design challenges for such antennas. When designing these antennas, the influence of human body on their characteristics (e.g., gain pattern distortion) has to be carefully accounted for; otherwise, performance degradations such as pattern fragmentation, power absorption and central frequency shift will occur [5,6]. For UWB simulations in this paper, we have used the loop antenna as shown in Fig. 3. This antenna has an operating frequency range of 3.1-5.1 GHz and its size is 29.25×38.5×1 mm. It is printed on a side of FR4 substrate with dielectric constant of $\varepsilon_r = 4.4$ and loss tangent of $tan\theta = 0.02$. Figure 4 displays the VSWR (Voltage Standing Wave Ratio) of the antenna in proximity to human body. Detailed study of the characteristics of this antenna in the free space and in direct contact with human body has been provided in [2,3].

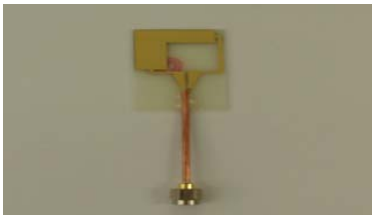

Figure 3. The UWB Loop Antenna

[1] HFSS is registered trademark of Ansoft Corporation. The HFSS has been used in this research to foster understanding. Such identification does not imply recommendation or endorsement by the National Institute of Standard and Technology, nor does it imply that this product is necessarily the best available for the purpose.

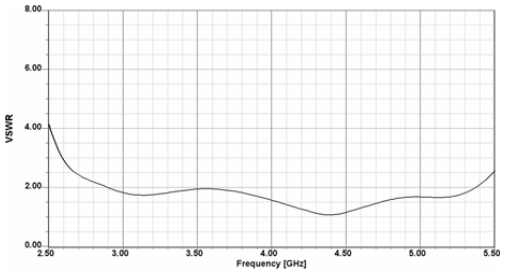

Figure 4. The UWB antenna VSWR in proximity to the body surface

IV. SIMULATION SCENARIOS & RESULTS

Figure 5 displays the relative positions of the receivers and transmitters in our simulation. The receiver positions are marked with red circles while the transmitter positions are marked with a green box. The receiver locations have been chosen accordingly to their potential medical application as suggested in [8]. They are left lower arm, left upper arm, left ear, head, right ear, shoulder, chest, right rib and left waist. The transmitter locations have been chosen according to potential placement of a gateway node such as a cell phone, PDA or a smart watch. They are stomach, right waist and left wrist. In all cases the transmitter antennas were located about 15 mm away from the body surface.

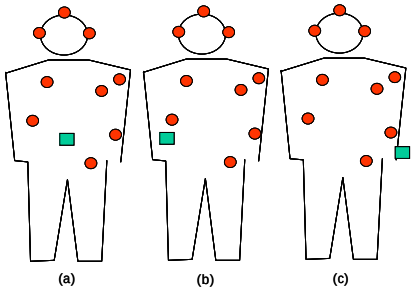

Figure 5. Various recievers locations for path loss calculation (a) transmitter on stomach (b) transmitter on right-side waist (c) transmitter on the left wrist

We first focused on scenarios shown in Fig. 5a. For each receiver location, the frequency response of the channel was calculated across the UWB frequency range of 3.1 to 5.1 GHz with a step size of 10 MHz. Figure 6 displays all 9 frequency responses corresponding to the 9 receiver locations in Fig. 5a. As observed, all channel responses are highly frequency dependent. Using IFFT with appropriate hamming window, we can obtain the temporal response of the channel. For example, Fig. 7 represents the normalized impulse response of the channel when the receiver is located on the right shoulder. The delay of the first arrival corresponds to the distance traveled by the UWB pulse. To calculate the distance based on the time of arrival, the exact speed of RF waves is needed. In this case, the velocity of RF wave is lower than that of free space (i.e. 3×10^8). The velocity is reduced by the square root of the permittivity of the body surface since relative permeability is close to 1. For example, for skin (i.e. dielectric permittivity of 36.5), the velocity of RF waves is approximately reduced by a factor of 6. For the example shown in Fig. 7, this translates to a distance of about 40 cm (i.e. 8 ns × 3 × 10^8/6) which happens to match the physical straight-line distance (i.e. 40.9 cm) between the transmitter and receiver in this case. In general, derivation of the distance based the arrival times is complicated as the exact speed of RF waves is hard to estimate for body surface propagation. Figure 8 shows the normalized impulse response of the channel when the receiver is located on the left wrist and the transmitter is located on the left waist. The two arrival components for this scenario possibly correspond to propagation through the air and propagation over the body surface.

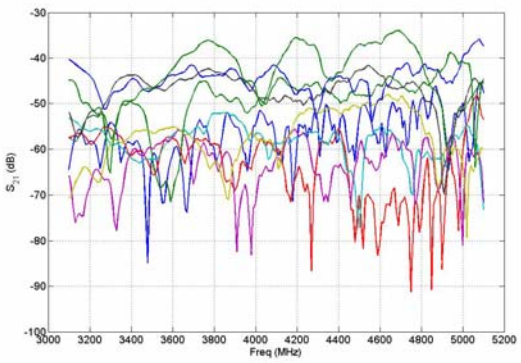

Figure 6. Frequency domain channel response at the 9 receiver locations

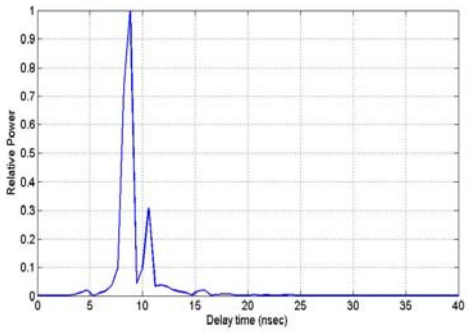

Figure 7. Impulse response: Stomach to right shoulder

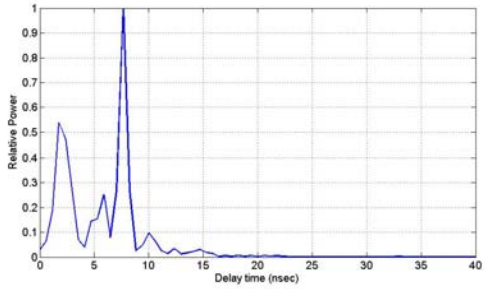

Figure 8. Impulse response: left wrist to left waist

We also calculated the path-loss between each receiver and the transmitter in Fig. 5a at each frequency in the range 3.1-5.1

GHz. The path-loss simply denotes the difference between the transmitted and received power; and therefore, it includes the antenna gains on both side. This is usually not the case for channel models corresponding to most wireless systems, but for BAN, the antenna gains are considered to be part of the channel [4]. This is due to the effect of the body surface on the antenna radiation pattern which makes its separation almost impossible.

The following simple statistical model has been used to characterize the path-loss.

$$PL(d) = PL(d_0) + 10n\log_{10}(d/d_0) + S \qquad d \geq d_0$$

d_0 is the reference distance (i.e., 50 mm), and n is the path-loss exponent which heavily depends on the environment where RF signal is propagating through. S is the random scatter around the mean and represents deviation in dB caused by different receiver/transmitter positions on the body and their antenna gains in different directions.

The path-loss exponent varies from 0.95 to 5.25 across the frequency band of 3.1-5.1 GHz. The average path-loss for each receiver location and the linear regression line for scenario 5a are shown in Fig. 7. The random scatters around the mean exhibit a Normal distribution with a standard deviation (σ_s) of about 2.4 dB (i.e. $S \sim N(0,\sigma_s^2)$). The obtained average path-loss exponent is 2.83 which is roughly in agreement with the physical experiment results reported in [10,11]. The slight difference could be due to the different antennas used in those studies and the UWB antenna that we have used in our simulation. We repeated our analyses for cases where transmitter was located at different positions (i.e. scenarios 5b and 5c). The extracted path-loss parameters are shown in Table 1. No significant variation in the average path-loss exponent is observed.

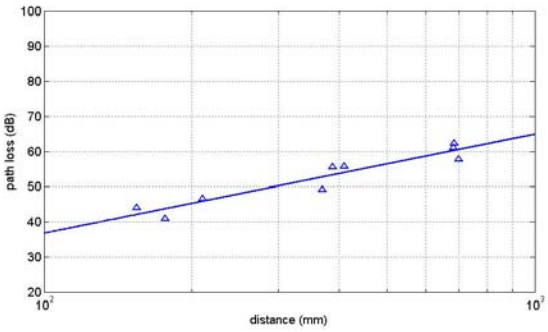

Figure 9. Path loss versus distance for the 9-point experiment averaged over 3.1-5.1 GHz

Transmitter Location	$PL(d_0)(dB)$	n	$\sigma_s(dB)$
Stomach	28.22	2.83	2.40
Right Waist	26.01	2.85	3.52
Left Wrist	18.90	2.98	3.70

Table 1. Parameters for the statistical path loss model for different transmitter locations

In the above process, the derivation of the path-loss parameters only involved 9 sample points. It would be interesting to find out whether a larger number of sample points would affect the resulting parameters. This could be generally difficult to ascertain with more physical experiment as it involves human subjects that have to stand still while participating in the experiment. However, we can easily consider the entire body surface and obtain a comprehensive scatter plot. For example, colors in Fig. 10 shows the path-loss over the entire body surface in our virtual reality platform when the transmitter is located on top of the stomach area. To obtain the path-loss parameters, here, we have only considered the front side of the body; since distance should denote over the body-surface distance as opposed to the straight line distance. This is because, at high frequencies, such as UWB, the through-body propagation is almost negligible; and therefore, we only need to consider over-the-surface propagation. This corresponds to over-the-surface distance between a transmitter and a receiver. As measuring the shortest distance between two points over the surface of the body (i.e. a 3D manifold) is not a trivial task, we have filtered out the sample points that are located in the back side of the body and used the approximation of straight-line distance for all sample points that are in the front side of the body.

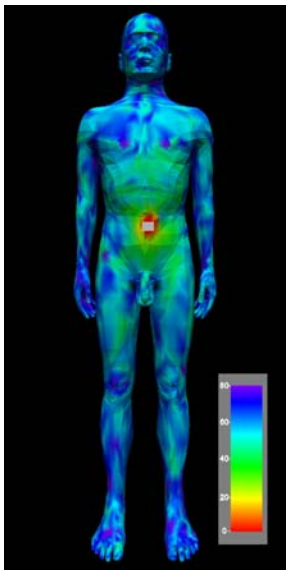

Figure 10. Path-loss over the body surface when the transmitter is loacted on the stomach

Figure 11 shows the scatter plot for the path-loss (at 4.1 GHz) as a function of TX-RX separation for the case when the transmitter is located on the stomach. The mean value of the random path-loss has been displayed by a solid line. This is obtained by fitting a least squares linear regression line through the scatter of measured path-loss sample points in dB such that the root mean square deviation of sample points about the regression line is minimized. This random scatters around the mean still shows a normal distribution with zero mean and

standard deviation of about 8.34 dB (see Fig. 9). The path-loss exponent has been reduced to 1.87.

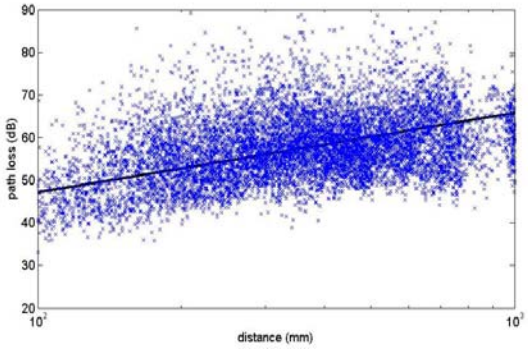

Figure 11. Scatter plot of the path-loss versus distance for body surface at 4.1 GHz when transmitter is located on the stomach

We repeated our analyses for cases where transmitter was located at different positions (i.e., scenarios in Figs. 5b and 5c). For example, the images in Figure 12 shows the path-loss on the body surface when the transmitter is located near the left wrist. Keep in mind that in order to have the right estimate for sample point distances, only the points that reside on the left side of the body have been used (see Fig. 13). Scatter plots corresponding to scenarios where transmitter is located on the right waist and left wrist have been omitted for brevity. The extracted path-loss parameters for these cases are shown in Table 2a.

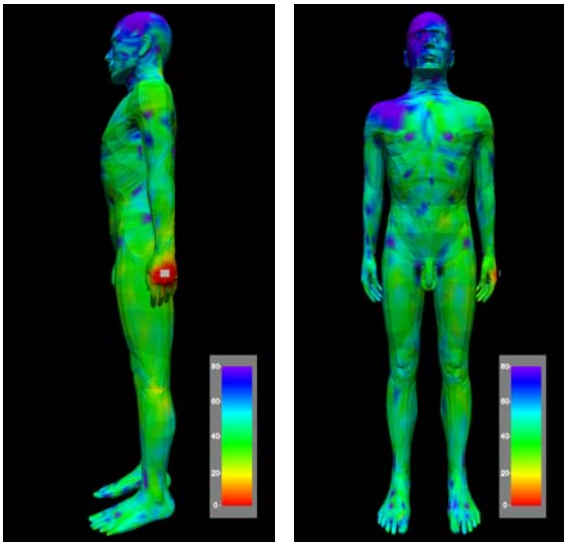

Figure 12. Path-loss over the body surface when the transmitter is loacted near the left wrist

The parameters in table 2a correspond to the transmit frequency of 4.1 GHz. To see whether there exists any dependency to the frequency, we also repeated the simulations for all three scenarios at frequencies of 3.3 and 4.7 GHz. Table 2b displays the extracted parameters at these frequencies for the case when the transmitter is located on the stomach.

Compared to the case when we only had 9 sample points, the path-loss exponent is lower in all cases in Table 2. One explanation for this could be the existence of creeping waves around the body surface. In our 3D simulations, we have observed that the directions of the Poynting vectors which represent the direction of energy flux of an electromagnetic field are mostly parallel to the body surface. This creeping wave phenomenon could facilitate the propagation of RF waves over the body surface; and therefore, lead to a better loss exponent for on-body channels. Further studies and analysis are needed to investigate this issue. One should keep in mind that layers of clothing could cause additional loss to the signal.

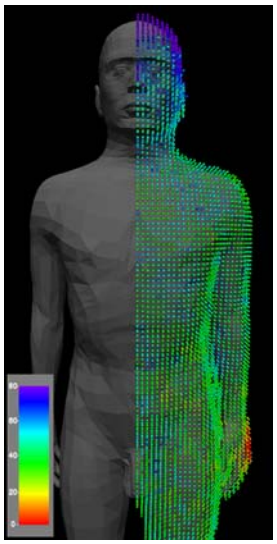

Figure 13. Sample points that reside on the left-side of the body

Transmitter Location	$PL(d_0)(dB)$	n	$\sigma_s(dB)$
Stomach	41.53	1.87	7.94
Right Waist	32.12	2.10	9.51
Left Wrist	25.24	1.91	9.72

(a)

Frequency	$PL(d_0)(dB)$	n	$\sigma_s(dB)$
3.3 GHz	45.77	1.64	8.34
4.1 GHz	41.53	1.87	7.94
4.7 GHz	38.57	1.40	7.87

(b)

Table 2. Parameters for the statistical path loss model (a) different transmitter locations (b) different frequencies

V. Conclusion

Using a 3D virtual reality simulation environment, here we have studied body-surface propagation for wearable sensors. In particular, we looked at the parameters of a simple statistical path-loss model and how they are affected when the number or location of the sample points change.

One difficulty in comparing the results of such simulations with actual measurements (or even comparing the results of two sets of measurements data obtained by two different sources) is the inclusion of the antenna characteristics in the channel model. The authors, therefore, plan to continue this study by focusing on results obtained from both simulations and measurements using the same antenna.

In general, studying body surface propagation for specific scenarios such as people wearing medical implants is also possible with our platform. The materials used in building the implant could affect the radio propagation from wearable sensors. Also, evaluating the efficiency of custom made antennas and comparing the results with other antennas can be easily done in our system. In addition, the 3D visualization platform is an ideal environment to observe and study the creeping wave propagation on the body surface. We plan to study this phenomenon and further information will be provided in a future publication.

More in-depth research on this subject is undoubtedly required to further understand the characteristics of radio frequency propagation for wearable sensors. The authors believe that the virtual reality environment introduced here creates a flexible platform to visualize and understand body-surface propagation which will be very useful in identifying and optimizing the necessary physical measurement campaign.

Acknowledgment

The authors would like to express their gratitude to Steven Satterfield of the Scientific Applications and Visualization Group for his assistance in the system setup and his ongoing contribution in the development of tools for the NIST immersive visualization system.

References

[1] J. G. Hagedorn, J. P. Dunkers, S.G. Satterfield, A. P. Peskin, J. T. Kelso, J. E. Terrill, "Measurement tools for the immersive visualization environment: Steps toward the virtual laboratory", Journal of research of the National Institute of Standard & Technology, Vol. 112, Num. 5, Sept.-Oct. 2007

[2] K. Y. Yazdandoost, R. Kohno, "Ultra Wideband L-loop antenna," IEEE International Conference on Ultra-Wideband, 2005

[3] K.Y.Yazdandoost, R.Kohno, "UWB Antenna for Wireless Body Area Network", Proceedings of Asia-Pacific Microwave Conference 2006

[4] G. Yang, "Body sensor networks", Springer-Verlag London Limited 2006, ISBN 1-84628-272-1

[5] P. S. Hall, Y. Hao, "Antennas and propagation for body centric wireless communications", Artech House, Inc. 2006, ISBN 1-58053-493-7

[6] C. Polk, E. Postow, "Biological effects of electromagnetic fields", CRC Press, Inc., 1996, ISBN 0-8493-0641-8

[7] K. Sayrafian-Pour, W. Yang, J. Hagedorn, J. Terrill, K. Y. Yazdandoost, "A Statistical Path Loss Model for Medical Implant Communication Channels", Proceedings of the IEEE PIMRC 2009

[8] K. Takizawa, T. Aoyagi, J. Takada, N. Katayama, K. Y. Yazdandoost, T. Kobayashi, R. Kohno, "Channel Models for Wireless Body Area Networks", Proceedings of the 30th Annual International IEEE EMBS Conference, August 20-24, 2008

[9] A. Fort, J. Ryckaert, C. Desset, P. Doncker, P. Wambacq, L. V. Biesen, "Ultra-Wideband Channel Model for Communication Around the Human Body", IEEE Journal on Selected Areas in Communications, Vol. 24, No. 4, April 2006

[10] A. Fort, C. Desset, J. Ryckaert, P. D. Doncker, L. V. Biesen, P. Wambacq, "Characterization of the Ultra Wideband Body Area Propagation Channel", Proc. ICU, Zurich, Switzerland, 2005, pp. 22-27

[11] T. Zasowski, F. Althaus, M. Stager, A. Wittneben, G. Troster, "UWB for Noninvasive Wireless Body Area Networks: Channel Measurements and Results", Proc. IEEE Conf. Ultra Wideband Syst. Technol., Nov. 2003, pp. 285-289